ISPRS Annals of the Photogrammetry, Remote Sensing and Spatial Information Sciences, Volume X-5/W2-2025
Unleashing the power of Geospatial & Frontier Technologies for a Sustainable Future – GIFTS Summit 2025,
1–3 September 2025, Symbiosis International University, Pune, India

High-Resolution Soil Moisture Mapping using MSAVI-LST based Triangle Method

Sonu Kumar[1,*], Rajendra Prasad[1], Jyoti Sharma[1,2], Bharatkumar S. Prajapati[1]

[1] Indian Institute of Technology (BHU), Varanasi, India [2] India Meteorological Department, New Delhi, India
* Corresponding author - sonukumar.rs.phy23@itbhu.ac.in

Keywords: Soil Moisture, Triangle Method, MSAVI, NDVI, Downscaling, Remote Sensing

Abstract

High-resolution soil moisture information is an essential parameter for hydrological, agricultural, and climatic processes. However, existing satellite products, such as SMAP, provide soil moisture at coarse resolution (9-36 km), limiting their regional utility. To address this, various studies have introduced downscaling techniques using optical and thermal data, but accounting for vegetation modulation remains a challenge. Therefore, in this study, an improvised downscaling approach based on the 'Triangle method' is used to estimate satellite soil moisture at 1 km spatial resolution from 9 km through the SMAP soil moisture product. Traditionally, this method uses the normalized difference vegetation index (NDVI) and Land Surface Temperature (LST) as an input for the downscaling approach. Here, the Modified Soil Adjusted Vegetation Index (MSAVI) is integrated as an alternative vegetation index to improve the vegetation sensitivity. The Triangle method has been used with first and second order of polynomial regression (1-1,1-2,2-1,2-2) relations between normalized vegetation index (VI*) and land surface temperature (LST*) to generate the soil moisture trapezoid for both NDVI and MSAVI. The validation of this methodology is carried out across different regions of Varanasi, on twelve dates of (2019-20,2023,2024,2025). Results indicate that the 1-1 polynomial order with MSAVI significantly outperforms the other combinations as well as the traditional NDVI-based approach. The highest correlation coefficient (R) of 0.76 with a minimum RMSE of 0.032 m^3/m^3 using MSAVI provides valuable insights for improving the downscaling technique of soil moisture in heterogeneous landscapes.

1. Introduction

Soil moisture (SM) is defined as the water held in the unsaturated soil zone, which plays an important role in weather prediction, flood forecasting, hydrological and energy cycles, drought assessment, scheduling of irrigation, forest fires, water resource management, and various climate- and agriculture-based modelling. It governs the various interactions between the land and atmospheric processes, (Petropoulos et al., 2015),(Bircher et al., 2012). Since soil moisture information plays a key role in various applications, its measurement is vast and widely used in research (Srivastava et al., 2021). Traditionally, in situ methods such as the gravimetric technique and time domain reflectometry (TDR), frequency domain reflectometry, the neutron probe method, and dielectric sensors have been used to measure soil moisture. However, these approaches are labor-intensive and require care, maintenance, proper handling, and calibration technique (Dobson et al., 2007) in some cases and are therefore impractical for large spatial and temporal scales. Although establishing a network of monitoring stations can expand coverage and provide continuous observations, it is expensive and requires significant maintenance. In addition, both methods produce only sparse point-based data, which are inadequate to represent the spatial heterogeneity of soil moisture on a broader scale. To cope with these difficulties, the satellite remote sensing method enables us to retrieve and monitor surface soil moisture on a global scale, which cannot be achieved by conventional methods (Gupta et al., 2022). For the appropriate monitoring of global soil moisture, the low-frequency microwave bands are the best due to their high penetration capability through vegetation and high sensitivity to surface soil moisture (Chaudhary et al., 2021). Vegetation has a more pronounced effect on the microwave signal at higher frequencies (Sharma et al., 2025). These days, L-band radiometers are used by NASA's SMAP and the European Space Agency's SMOS missions to measure worldwide soil moisture at spatial resolutions of 36–40 km. To better understand hydrological processes and forecast how SM fluctuations may affect weather patterns, environmental processes, and climate change, spatial resolution must be improved. SMAP was initially paired with an L-band radiometer with a 36-kilometer spatial resolution and an L-band radar with a 3-km spatial resolution in order to boost the radiometer's spatial resolution from 36 km to 9 km. However, after three months, the radar stopped working, leaving only the radiometer data (West, 2014). Despite the availability of multiple satellite missions dedicated to soil moisture retrieval (SMAP, SMOS, AMSR2), their coarse resolution doesn't meet the needs of many localized applications such as precision agriculture, watershed hydrology, and drought risk assessment (Mishra et al., 2015). In many regions, sub-kilometer variations in soil moisture are driven by fine-scale differences in land use, vegetation cover, and irrigation practices, which remain unresolved by these sensors. Moreover, the temporal mismatch between satellite overpass frequency and the dynamic nature of surface soil moisture further complicates its direct use at the field scale. To address these limitations, different downscaling approaches have been developed to meet the applications that use soil moisture at a finer scale (Das et al., 2013), (Merlin et al., 2012), (Agarwal et al., 2025), (Kim et al., 2018). The triangle method is based on the merging of thermal and optical data and offers a semi-empirical yet physically interpretable framework for estimating and downscaling soil moisture using satellite-driven land surface temperature (LST) and vegetation indices (VIs). Traditionally, (Gillies and Carlson, 1995) and Gillies (Wang and Qu, 2009) demonstrated that there is a unique relationship among soil moisture, the NDVI, and the LST for a specific study area, which can be identified as a "Universal Triangle." However, NDVI may saturate under dense vegetation and be less sensitive to soil, par-

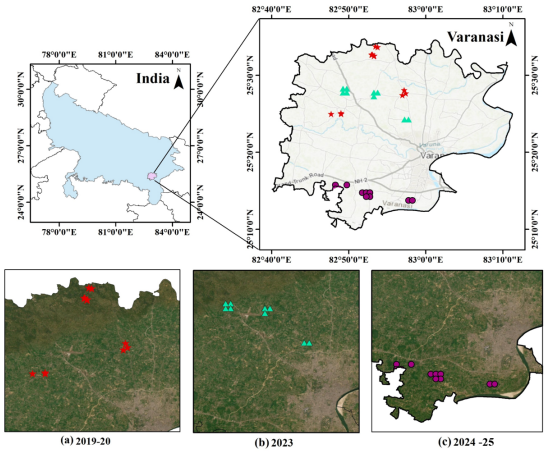

Figure 1. Ground data of Varanasi region figure (a, b, c) data points of 2019-20, 2023, and 2024-25, respectively

ticularly in semi-arid vegetation areas. This study proposes using the Modified Soil Adjusted Vegetation Index (MSAVI) as an alternative to NDVI with different orders of polynomial regression relationships between vegetation index (VI) and land surface temperature (LST) to improve the optimization of soil moisture at 1 km resolution and help to refine the triangle method to achieve better accuracy in satellite-based SM downscaling. The integration of MSAVI as a vegetation index with thermal data highlights the importance of selecting a suitable vegetation index, order, and model configuration for improving the downscaling accuracy of the Triangle method.

2. Study area and Dataset

2.1 Study Area

The Varanasi district of Uttar Pradesh, India, is selected for the study region due to its agro-climatic diversity and heterogeneous land covers. The region is geographically located at 25°18'45" N, 82°58'15" E, situated about 50-70 feet from river level. Since it is a part of the Indo-Gangetic plains, characterized by fertile alluvial soil regularly enriched by seasonal floods, over 60% of the area is agriculture-based, with major crops including wheat, pearl millet, paddy, and maize. Heterogeneous land cover type and humid subtropical climate condition makes Varanasi a s ideal location for testing soil moisture downscaling methods, especially those reliant on the LST-vegetation index relationship, such as the triangle method. Figure 1 shows the study areas of in-situ observations.

2.2 Data Used

2.2.1 Ground observations The in-situ observations were collected using the HydraGo, a portable probe,known for its accuracy and durability in soil moisture monitoring (Bhanumathi and Kalaivanan, 2018). It simultaneously measures the soil moisture, soil temperature, and dielectric constant using the principle of the coaxial impedance dielectric reflectometry method. Measurements were conducted over 12 different dates between 2019 and 2025, covering various seasonal conditions to ensure diverse soil moisture scenarios. Figure 1 illustrates the sampling points, and for each sampling date, between nine and nineteen grids were selected, each of which represents a 1

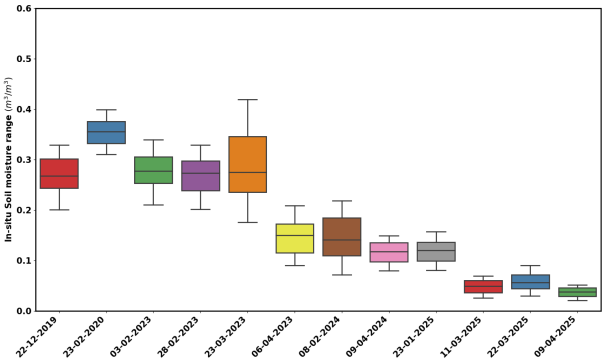

Figure 2. Soil moisture values correspond to different dates

km x 1 km area, and in each of them, 20 to 25 data points were collected for local heterogeneity and to minimize random errors. The geographic location and sampling locations for each date are detailed in Table 1. Figure 2 displays the soil moisture range across the twelve dates. The lower soil moisture was recorded during March-April, corresponding to the onset of the summer season, when rising temperatures and reduced precipitation contribute to drier soil conditions. In the remaining months, the observed soil moisture ranges from 0.2 to 0.45, reflecting the cooler winter season when soil retains more moisture.

No.	Date	Grids	Points/ Grid
1	22-12-2019	12	21
2	23-02-2020	12	21
3	03-02-2023	9	23
4	28-02-2023	9	23
5	23-03-2023	9	23
6	06-04-2023	9	23
7	08-02-2024	11	25
8	09-04-2024	11	25
9	23-01-2025	19	22
10	11-03-2025	19	22
11	22-03-2025	19	22
12	09-04-2025	19	22

Table 1. Summary of *in situ* soil moisture Observations

2.2.2 SMAP Data The SMAP project, launched in January 2015 and began operations in April of the same year, is an orbiting observatory that measures the amount of water in surface soil all over the world. Before its power supply failed in July 2015, the radar gathered scientific data for more than three months. But the radiometer continues functioning and delivering passive radiometric data at multiple levels of detail (1 km, 9 km, and 36 km) and time frames (daily or multi-day) for this data. This study used SMAP L1 TB E data packages, which provide the brightness temperature on a daily temporal resolution and at 9 km spatial resolution. The SMAP L1C TB E data were used to estimate the SM content, which was then downscaled utilizing downscaling methods. Furthermore, the MYD11A1 and MOD09GA products, which are captured by the MODIS sensor on the Aqua and Terra satellites, are accessible via the MODIS Land Processes Distributed Active Archive Center (LPDAAC) website (https://lpdaac.usgs.gov/). The Aqua satellite collects data at around 1:30 AM/PM, whilst the Terra satellite does so at around 10:30 AM/PM. The MOD09GA product provides Terra MODIS surface spectral reflectance data with a resolution of 500 m, whereas the MYD11A1 product provides daily LST images with a spatial resolution of 1 km. Daily vegetation indices like NDVI and MSAVI were specifically calculated using Bands 1 (red) and 2 (NIR) of the MOD09GA.

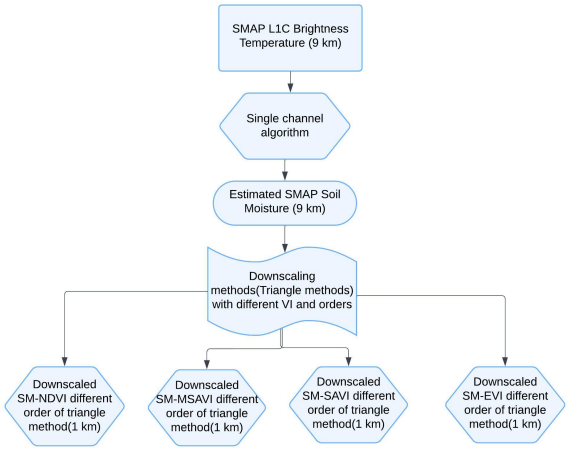

Figure 3. Sketch illustrating the integration of SCA into the SMAP soil moisture downscaling procedure.

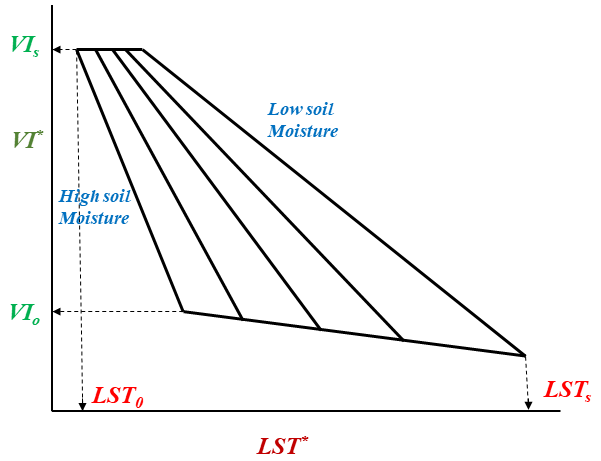

Figure 4. Triangular relationship between SM, LST, and VIs

The MODIS LST and reflectance images were reprojected and resampled using the MODIS Reprojection Tool (MRT). Although the majority of the research dates were cloud-free, cloud-affected areas were filtered out using the efficacy flags from the MODIS LST product to guarantee that only high-quality data was used. According to (Mathew et al., 2018), the program also assisted in correcting LST photos by pixels that were of low quality, with an acceptable error margin of ±2 K in LST readings. Measurements of ground soil moisture were taken between 8:00 and 11:00 a.m. local time in order to match satellite overpass times as precisely as possible. Around 6:00 AM local time is when SMAP descending overpasses take place, and around 10:30 AM is when MODIS Terra gathers data. By choosing days with bright skies and consistent morning conditions, the tiny temporal mismatch was reduced. Furthermore, this time difference is thought to have little effect on downscaling precision because the triangle approach depends on spatial correlations rather than exact temporal values.

3. Methodology

The downscaling of SMAP soil moisture data using multiple orders of the triangle approach using MSAVI and NDVI as vegetation indices is the main objective of this study. In this study, the single-channel algorithm (SCA) method was employed to obtain SM estimates from the SMAP satellite. The SM was then downscaled from 9 km to 1 km using these estimates. The complete study workflow is depicted in Figure 3.

3.1 Soil moisture estimation

The connection between microwave emission from the soil surface, plant, and atmosphere is explained by the tau-omega model. Omega is the single scattering albedo, which shows the proportion of microwave radiation scattered by the vegetation relative to the total energy that the vegetation layer intercepts, and tau is vegetation optical depth (VOD), which shows how much microwave radiation is attenuated by the vegetation (Gupta et al., 2016). SCA, based on the tau-omega model, can be expressed as (1) (Sharma et al., 2021), (Srivastava et al., 2014)

$$TB_p = (1-\gamma)(1-\omega)(1+r_p\gamma)T_v + (1-r_p)T_g \quad (1)$$

where TB_P, T_V, and T_g represent the brightness temperature, the vegetation temperatures, and the soil surface temperatures, respectively. Due to a lack of precise data, it has been widely thought that the temperatures of the soil surface and plants are almost equal. This effective temperature was determined using MODIS LST. For croplands, the scattering albedo (omega) is assumed to be 0.05. The subscript P denotes the polarization (H or V).

$$\gamma = \exp\left(-\tau/\cos\theta\right) \quad (2)$$

$$r_P(\theta) = r_{0P}(\theta)\exp\left(-h\cos^2\theta\right) \quad (3)$$

where tau (vegetation opacity) is given by $tau = b * \text{VWC}$ (vegetation water content), and the parameter b depends on frequency and vegetation. The estimated value of b is 0.25 ± 0.12 (Van de Griend and Wigneron, 2004) for the L-band microwave region. VWC data downloaded from SMAP L2 SM P E. In equations (2) and (3), θ represents the incident angle, while h in equation (3) refers to the surface roughness, which ranges from 0.1 to 0.4 for various land cover types and for L-band frequency. For the given study region, a roughness parameter range of 0.2 to 0.3 is appropriate (Sharma et al., 2021). The reflectivity for a smooth surface, $r_0(\theta)$, can be calculated using Fresnel's equations (Jagdhuber, 2016).

$$r_{oH} = \left|\frac{\cos\theta - \sqrt{\varepsilon - \sin^2\theta}}{\cos\theta + \sqrt{\varepsilon - \sin^2\theta}}\right|^2 \quad (4)$$

$$r_{oV} = \left|\frac{\varepsilon\cos\theta - \sqrt{\varepsilon - \sin^2\theta}}{\varepsilon\cos\theta + \sqrt{\varepsilon - \sin^2\theta}}\right|^2 \quad (5)$$

In equations (4) and (5), ε represents the soil dielectric constant, which is influenced by SM, surface temperature, and soil texture. This value is calculated using a dielectric model that takes temperature and texture into account, as developed by Mironov et al (Mironov et al., 2012) The estimated SMAP soil moisture (est_SM) through SCA is further used as the input for different orders of the triangle method with NDVI and MSAVI.

3.2 Soil Moisture Downscaling Using Different Orders of the Triangle Method

A technique for estimation of SM based on regional temperature and vegetation index variations has been presented by Carlson (Carlson, 2007). Later, the same triangle technique connection was applied to downscale and estimate high-resolution SM using LST and VI. High-resolution LST and VI are used to

regress this triangle method connection backward in order to estimate high-resolution SM. Polynomial regression relationships can be used to express the relationship, such as (Zhao and Li, 2015), (Kim et al., 2018).

$$SM = \sum_{i=0}^{n}\sum_{j=0}^{m} a_{ij} VI^{*(i)}\, LST^{*(j)} \tag{6}$$

In this case, SM stands for soil moisture, and LST^* and VI^* are defined as the normalized LST and VI, respectively.

$$LST^* = \frac{LST - LST_{min}}{LST_{max} - LST_{min}} \tag{7}$$

$$VI^* = \frac{VI - VI_{min}}{VI_{max} - VI_{min}} \tag{8}$$

The minimum and maximum values of LST and VI calculated over the chosen research region are indicated by the min and max subscripts, respectively. This study used the triangle approach with various orders of polynomial relations to compute regression coefficients a_{ij}. Here, the original SM, VI, and LST were replaced with coarse-resolution SM, VI (9 km), and LST (9 km), respectively.

$$SM_c = \sum_{i=0}^{n}\sum_{j=0}^{m} a_{ij}\, VI_{9km}^{*(i)}\, LST_{9km}^{*(j)} \tag{9}$$

LST^*_{9km} and VI^*_{9km} are the aggregated values of MODIS LST^* (1 km) and VI^* (500 m), respectively, that were determined using an arithmetic mean. The high-resolution SM was then assessed using the predicted regression coefficients in conjunction with the 1-km MODIS LST and NDVI.

$$SM_{High} = \sum_{i=0}^{n}\sum_{j=0}^{m} a_{ij}\, VI_{1km}^{*(i)}\, LST_{1km}^{*(j)} \tag{10}$$

For a 1-1 order polynomial, i = 1 and j = 1, the relation is given as follows:

$$SM = a_{00} + a_{10}VI^* + a_{01}LST^* \tag{11}$$

For a 1-2 order polynomial, i = 1 and j = 2, the relation is given as follows:.

$$SM = a_{00} + a_{10}VI^* + a_{01}LST^* + a_{11}VI^*LST^* + a_{02}LST^{*2} \tag{12}$$

For 2-1 order polynomial, i = 2 and j = 1, the relation can be given as follows:

$$SM = a_{00} + a_{10}VI^* + a_{01}LST^* + a_{11}VI^*LST^* + a_{20}VI^{*2} \tag{13}$$

And for 2-2 order polynomial, i = 2 and j = 2, the relation can be given as follows:

$$SM = a_{00} + a_{10}VI^* + a_{01}LST^* + a_{11}VI^*LST^* + a_{20}VI^{*2} + a_{02}LST^{*2} \tag{14}$$

Here a_{00},a_{10},a_{01},a_{11},a_{20},a_{02} are regression parameters for different orders of the triangle method. In this study, NDVI and MSAVI (Qi et al., 1994) are used as vegetation indices, and their results are further compared. The NDVI and MSAVI can be calculated as

$$NDVI = \frac{(NIR - RED)}{(NIR + RED)} \tag{15}$$

$$MSAVI = \frac{2 \times NIR + 1 -}{2} \times \left[1 - \sqrt{1 - \frac{8 \times (NIR - RED)}{(2 \times NIR + 1)^2}}\right] \tag{16}$$

4. Results

4.1 Performance analysis of the soil moisture downscaling algorithm for different orders of the triangle method using NDVI:

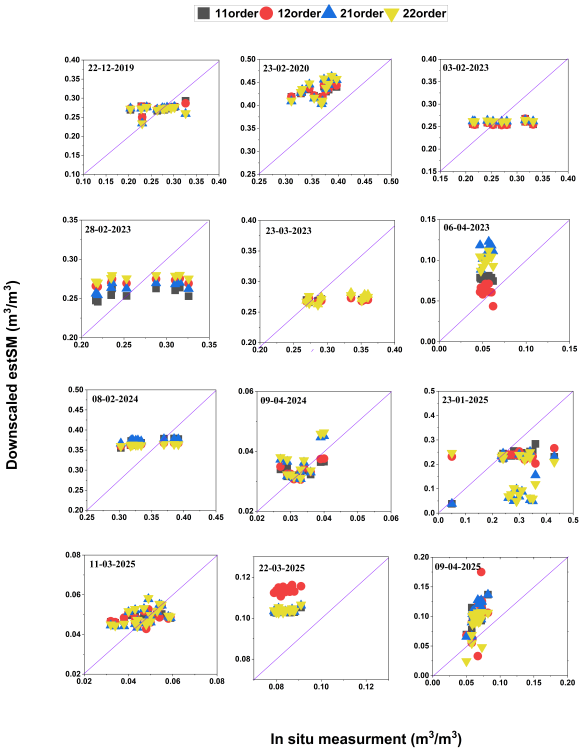

Figure 5. Comparison of Ground data and Downscaled est_SM for twelve dates using NDVI as vegetation index

The downscaled SMAP soil moisture (SM) product was compared with in-situ measurements to analyse the performance of downscaled SM using the triangle method with different polynomial orders (11, 12, 21, 22) and NDVI as a vegetation index. Figure 5 represents the scatter plots of the comparisons across twelve dates, and Table 2 summarizes the performance metrics—RMSE, correlation coefficent (R), and bias. The findings show that, in terms of accuracy, lower-order models perform better than higher-order ones. The most accurate SM downscale is provided by the 11 order, which has the lowest RMSE of 0.0377 m^3/m^3. The RMSE increases with increasing order, showing lower accuracy at higher orders: 0.0514 m^3/m^3 for the 12 order, 0.0487 m^3/m^3 for the 21 order, and 0.0606 m^3/m^3 for the 22 order. A comparable pattern is shown by

No.	Date	1-1 Order			1-2 Order			2-1 Order			2-2 Order		
		RMSE (m^3/m^3)	Bias (m^3/m^3)	R	RMSE (m^3/m^3)	Bias (m^3/m^3)	R	RMSE (m^3/m^3)	Bias (m^3/m^3)	R	RMSE (m^3/m^3)	Bias (m^3/m^3)	R
1	22-12-2019	0.031	0.004	0.555	0.032	0.005	0.501	0.034	0.001	0.190	0.034	0.001	0.221
2	23-02-2020	0.072	0.069	0.529	0.074	0.070	0.474	0.076	0.071	0.444	0.078	0.074	0.502
3	03-02-2023	0.048	-0.018	0.626	0.041	-0.014	0.460	0.041	-0.008	0.421	0.048	-0.013	0.541
4	28-02-2023	0.039	-0.011	0.562	0.040	0.004	0.562	0.038	-0.002	0.590	0.123	-0.109	0.555
5	23-03-2023	0.053	-0.040	0.704	0.055	-0.041	0.320	0.050	-0.038	0.733	0.053	-0.034	0.500
6	06-04-2023	0.024	0.024	-0.113	0.013	0.008	-0.417	0.056	0.055	0.519	0.046	0.045	0.315
7	08-02-2024	0.041	0.338	0.726	0.041	-0.011	0.687	0.044	0.036	0.751	0.103	0.095	0.721
8	09-04-2024	0.003	0.005	0.583	0.003	0.001	0.616	0.005	0.002	0.634	0.005	0.003	0.633
9	23-01-2025	0.0766	-0.061	0.798	0.093	-0.058	0.668	0.172	-0.142	0.285	0.1793	-0.134	-0.200
10	11-03-2025	0.0068	0.0015	0.513	0.006	0.0024	0.520	0.006	0.0020	0.487	0.0069	0.0025	0.476
11	22-03-2025	0.019	0.019	0.526	0.032	0.0300	0.463	0.0197	0.1954	0.533	0.0201	0.0199	0.499
12	09-04-2025	0.039	0.037	0.645	0.189	0.095	0.470	0.042	0.040	0.781	0.031	0.023	0.468
Mean	–	0.0377	0.0306	0.6152	0.0514	0.0119	0.5218	0.0487	0.0177	0.5307	0.0606	-0.0022	0.4937

Table 2. RMSE, Bias, and Correlation coefficient (R) Across Different Orders for NDVI

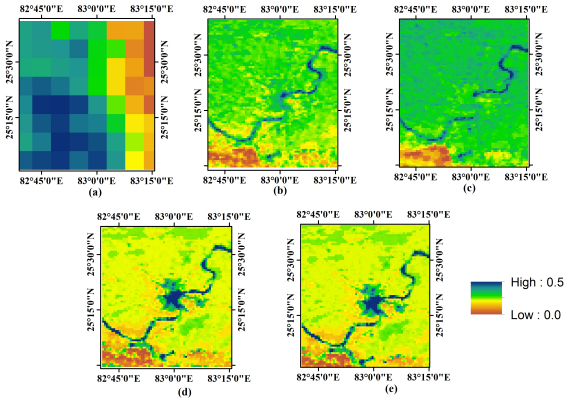

Figure 6. Spatial maps of (a) est_SM and downscaled est_SM using (b) 11 order, (c) 12 order, (d) 21 order, and (e) 22 order of the triangle method for NDVI as a vegetation index

correlation coefficients (R). When the negative outliers for 6 April 2023 (-0.113, -0.417) and 23 January 2025 (-0.200) are removed, the average R for the 11 order rises to 0.6152. R rises to 0.5218 for the 12 order when outliers are removed. The correlation strength decreases with increasing order, as indicated by the adjusted R values for the 11, 12, 21, and 22 orders, which are 0.6152, 0.5218, 0.5307, and 0.4937, respectively. The range of bias values is 0.0377 m^3/m^3 (11 order) to -0.0022 m^3/m^3 (22 order). The 11 order's slightly larger bias is offset by its better RMSE and R performance, whereas the 22 order has the lowest bias, indicating high reliability. The spatial improvement in SM maps is seen in Figure 6. Compared to the original 9-km resolution SM map, the downscaled pictures for NDVI (11 to 22 orders) offer more detail, especially around features like the Ganges River close to Varanasi. The river and the vegetation areas are more clearly apparent at the 11th order, indicating improved spatial representation. In conclusion, the 11 order is the most efficient for SM downscaling, obtaining the lowest RMSE and maximum R. Lower-order models are more appropriate for downscaled SM applications, as higher orders lead to decreasing accuracy and correlation.

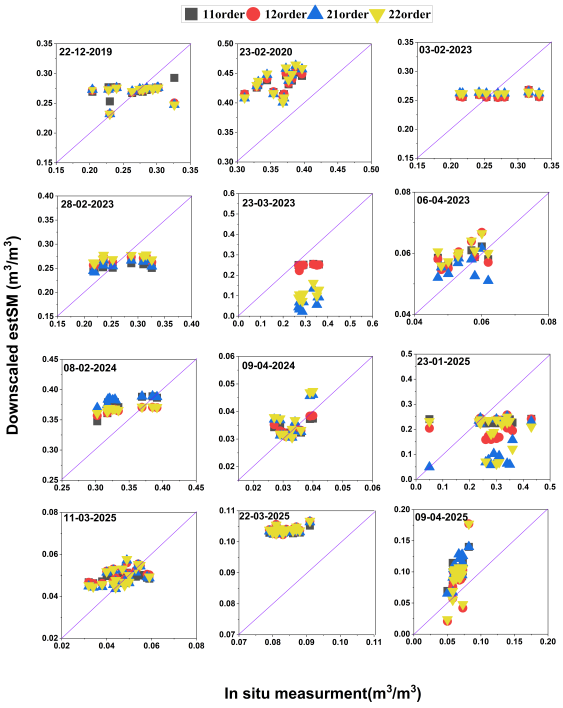

Figure 7. Comparison of Ground data and Downscaled est_SM for twelve dates using MSAVI as vegetation index

No.	Date	1-1 Order			1-2 Order			2-1 Order			2-2 Order		
		RMSE (m^3/m^3)	Bias (m^3/m^3)	R	RMSE (m^3/m^3)	Bias (m^3/m^3)	R	RMSE (m^3/m^3)	Bias (m^3/m^3)	R	RMSE (m^3/m^3)	Bias (m^3/m^3)	R
1	22-12-2019	0.031	0.004	0.572	0.033	0.004	0.342	0.036	-0.001	0.103	0.037	-0.001	0.061
2	23-02-2020	0.073	0.078	0.520	0.075	0.072	0.520	0.077	0.025	0.073	0.078	0.075	0.480
3	03-02-2023	0.048	-0.017	0.618	0.048	-0.017	0.618	0.048	-0.013	0.552	0.049	-0.013	0.550
4	28-02-2023	0.040	-0.013	0.562	0.037	-0.001	0.562	0.037	-0.009	0.581	0.037	0.004	0.570
5	23-03-2023	0.070	-0.060	0.690	0.071	-0.063	0.481	0.244	-0.240	0.630	0.200	-0.200	0.650
6	06-04-2023	0.006	0.005	0.560	0.007	0.005	0.537	0.007	0.005	0.530	0.036	0.036	0.636
7	08-02-2024	0.044	0.039	0.708	0.040	0.030	0.760	0.039	0.020	0.708	0.051	0.045	0.740
8	09-04-2024	0.003	0.001	0.580	0.003	0.001	0.630	0.005	0.003	0.640	0.006	0.003	0.640
9	23-01-2025	0.0955	-0.0603	0.728	0.1137	-0.084	0.1717	0.1676	-0.1389	0.2822	0.1413	0.099	0.0797
10	11-03-2025	0.0068	0.0016	0.5173	0.0070	0.0032	0.5343	0.0066	0.0021	0.5020	0.0068	0.0026	0.4893
11	22-03-2025	0.0197	0.0195	0.5235	0.0202	0.0200	0.4435	0.0198	0.0196	0.5350	0.0201	0.0200	0.4966
12	09-04-2025	0.039	0.038	0.663	0.037	0.026	0.605	0.043	0.014	0.788	0.0374	0.027	0.641
Mean	–	0.0396	0.0029	0.7603	0.0409	-0.0003	0.5170	0.0608	-0.0019	0.5276	0.0558	0.0106	0.5028

Table 3. RMSE, Bias, and Correlation coefficient (R) Across Different Orders for MSAVI

4.2 Performance analysis of the soil moisture downscaling algorithm for different orders of the triangle method using MSAVI:

Scatter plots comparing in situ and downscaled soil moisture (SM) data over a twelve-date period using MSAVI as the vegetation index are shown in Figure 7. Performance tables for the Triangle approach over four polynomial orders (11, 12, 21, and 22) are shown in Table 3 as RMSE, correlation coefficient (R), and bias.

For the 11, 12, 21, and 22 orders, the mean RMSE values are 0.0396 m^3/m^3, 0.0406 m^3/m^3, 0.0608 m^3/m^3, and 0.0558 m^3/m^3, respectively. The 21 order records the highest RMSE (0.0608 m^3/m^3), suggesting poorer performance, while the 11 order has the lowest RMSE (0.0396), showing higher accuracy in SM downscaling.The trend of correlation coefficients (R) is similar, with the greatest value of 0.7634 for the 11 order, indicating a closer connection between in situ and downscaled SM. The 22 order has the lowest R of 0.5028, indicating a poorer association, whereas the 12 order has a slightly lower R of 0.517. The range of bias values is -0.0003 m^3/m^3 (12 order) to 0.0029 m^3/m^3 (11 order). The 12 order exhibits the least bias (-0.0003 m^3/m^3), but its overall efficacy is reduced by its subpar RMSE and R values. The most dependable arrangement is the 11 order, which successfully balances the contributions of MSAVI and LST and has the highest R and lowest RMSE. The downscaled SM maps for MSAVI are shown in Figure 8. In comparison to higher orders, the Ganges River and vegetated areas are clearly apparent in the 11th order, demonstrating improved spatial representation. SM values increase with increasing order, while spatial detail decreases, particularly in landscapes that are heterogeneous. All things considered, the MSAVI 11 order performs the best, obtaining the lowest RMSE and highest R. On the other hand, the 21 order performs the poorest because of its greater RMSE and worse correlation, which are probably the result of placing too much weight on MSAVI in comparison to LST.

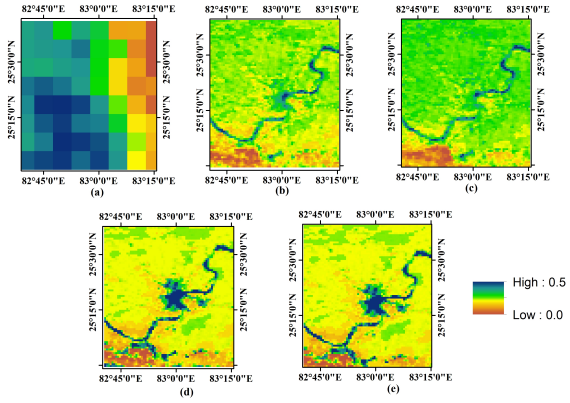

Figure 8. Spatial maps of (a) est_SM and downscaled est_SM using (b) 11 order, (c) 12 order, (d) 21 order and (e) 22 order of triangle method for MSAVI as a vegetation index

5. Cumulative comparison of performance of NDVI and MSAVI for different orders of the triangle method

A cumulative evaluation between MSAVI and NDVI across different orders of the triangle method is summarized in Table 4. The MSAVI consistently outperforms NDVI across most orders, especially in 1-1 order, where it achieves the highest correlation coefficient (R=0.7603) and lowest RMSE (0.0396 m^3/m^3) and a minimal bias of 0.0029 m^3/m^3, enhancing its reliability. The correlation coefficient (R) decreases and RMSE increases for further orders with R=0.5170 and RMSE= 0.0409 m^3/m^3 for 1-2 order, R=0.5276 and RMSE= 0.0608 m^3/m^3 for 2-1 order, and R=0.5028 and RMSE= 0.0558 m^3/m^3 for 2-2 order of MSAVI. The NDVI achieves a maximum of 0.6152 in correlation coefficient order and a minimum RMSE of 0.0377 m^3/m^3 in 1-1 order, followed by R=0.5218 and RMSE= 0.0514 m^3/m^3 for 1-2 order, R=0.5307 and RMSE= 0.0487 m^3/m^3 for 2-1 order, and R=0.4937 and RMSE= 0.0606 m^3/m^3 for 2-2 order. The bias for both MSAVI and NDVI does not follow a regular trend for all the orders, but their minimum values across all orders suggest minimal systematic errors in prediction. In summary, these results affirm the robustness of MSAVI in accounting for the downscaling approach, making it more reliable than NDVI, particularly in heterogeneous landscapes.

6. Conclusion

The use of the Modified Soil Adjusted Vegetation Index (MSAVI) as an alternative to the Normalized Difference Vegetation Index (NDVI) significantly improves the results of downscaling of the SMAP soil moisture product from 9 km to 1 km resolution in the 'Triangle Method' approach. NDVI, while widely

No.	VI	1-1 Order			1-2 Order			2-1 Order			2-2 Order		
		RMSE (m^3/m^3)	Bias (m^3/m^3)	R	RMSE (m^3/m^3)	Bias (m^3/m^3)	R	RMSE (m^3/m^3)	Bias (m^3/m^3)	R	RMSE (m^3/m^3)	Bias (m^3/m^3)	R
1	NDVI	0.0377	0.0306	0.6152	0.0514	0.0119	0.5218	0.0487	0.0177	0.5307	0.0606	-0.0022	0.4937
2	MSAVI	0.0396	0.0029	0.7603	0.0409	-0.0003	0.5170	0.0608	-0.0019	0.5276	0.0558	0.0106	0.5028

Table 4. RMSE, Bias (in m^3/m^3), and Correlation coefficient (R) for Different Orders of NDVI and MSAVI

used, tends to saturate in densely vegetated regions and is less sensitive to soil background reflectance in areas with sparse vegetation cover, leading to less reliable representations for the surface conditions. However, MSAVI addresses these limitations by incorporating a soil adjustment factor that enhances the sensitivity towards vegetation in low cover conditions. This makes MSAVI effective particularly in mixed land-use regions like Varanasi, where cropland, bare soil, and seasonal variations in vegetation coexist. By providing a more stable and accurate relationship between vegetation cover and land surface temperature (LST), MSAVI improves the structure of the trapezoidal space used in the triangle method, leading to better discrimination between wet and dry edges. Consequently, this results in lower RMSE, reduced bias, and higher correlation coefficients, as observed in the validation with in-situ soil moisture measurements.The enhanced performance of MSAVI facilitates more accurate and robust high-resolution soil moisture estimation across different seasons and land cover types.

References

Agarwal, V., Vishvendra Raj Singh, B., Marsh, S., Qin, Z., Sen, A., Kulhari, K., 2025. Integrated Remote Sensing for Enhanced Drought Assessment: A Multi-Index Approach in Rajasthan, India. *Earth and Space Science*, 12(2), e2024EA003639.

Bhanumathi, V., Kalaivanan, K., 2018. The role of geospatial technology with iot for precision agriculture. *Cloud Computing for Geospatial Big Data Analytics: Intelligent Edge, Fog and Mist Computing*, Springer, 225–250.

Bircher, S., Skou, N., Kerr, Y. H., 2012. Validation of SMOS L1C and L2 products and important parameters of the retrieval algorithm in the Skjern River Catchment, Western Denmark. *IEEE Transactions on Geoscience and Remote Sensing*, 51(5), 2969–2985.

Carlson, T., 2007. An overview of the" triangle method" for estimating surface evapotranspiration and soil moisture from satellite imagery. *Sensors*, 7(8), 1612–1629.

Chaudhary, S. K., Gupta, D. K., Srivastava, P. K., Pandey, D. K., Das, A. K., Prasad, R., 2021. Evaluation of radar/optical based vegetation descriptors in water cloud model for soil moisture retrieval. *IEEE sensors journal*, 21(18), 21030–21037.

Das, N. N., Entekhabi, D., Njoku, E. G., Shi, J. J., Johnson, J. T., Colliander, A., 2013. Tests of the SMAP combined radar and radiometer algorithm using airborne field campaign observations and simulated data. *IEEE Transactions on Geoscience and Remote Sensing*, 52(4), 2018–2028.

Dobson, M. C., Ulaby, F. T., Hallikainen, M. T., El-Rayes, M. A., 2007. Microwave dielectric behavior of wet soil-Part II: Dielectric mixing models. *IEEE Transactions on geoscience and remote sensing*, 35–46.

Gillies, R. R., Carlson, T. N., 1995. Thermal remote sensing of surface soil water content with partial vegetation cover for incorporation into climate models. *Journal of Applied Meteorology and Climatology*, 34(4), 745–756.

Gupta, D. K., Prashar, S., Singh, S., Srivastava, P. K., Prasad, R., 2022. Introduction to radar remote sensing. *Radar Remote Sensing*, Elsevier, 3–27.

Gupta, D., Prasad, R., Srivastava, P., Islam, T., 2016. Nonparametric model for the retrieval of soil moisture by microwave remote sensing. *Satellite Soil Moisture Retrieval*, Elsevier, 159–168.

Jagdhuber, T., 2016. An approach to extended Fresnel scattering for modeling of depolarizing soil-trunk double-bounce scattering. *Remote Sensing*, 8(10), 818.

Kim, D., Moon, H., Kim, H., Im, J., Choi, M., 2018. Intercomparison of downscaling techniques for satellite soil moisture products. *Advances in Meteorology*, 2018(1), 4832423.

Mathew, A., Khandelwal, S., Kaul, N., 2018. Investigating spatio-temporal surface urban heat island growth over Jaipur city using geospatial techniques. *Sustainable Cities and Society*, 40, 484–500.

Merlin, O., Rudiger, C., Al Bitar, A., Richaume, P., Walker, J. P., Kerr, Y. H., 2012. Disaggregation of SMOS soil moisture in Southeastern Australia. *IEEE Transactions on Geoscience and Remote Sensing*, 50(5), 1556–1571.

Mironov, V., Kerr, Y., Wigneron, J.-P., Kosolapova, L., Demontoux, F., 2012. Temperature-and texture-dependent dielectric model for moist soils at 1.4 GHz. *IEEE Geoscience and Remote Sensing Letters*, 10(3), 419–423.

Mishra, V. N., Prasad, R., Kumar, P., Gupta, D. K., Dikshit, P. K. S., Dwivedi, S. B., Ohri, A., 2015. Evaluating the effects of spatial resolution on land use and land cover classification accuracy. *2015 International Conference on Microwave, Optical and Communication Engineering (ICMOCE)*, IEEE, 208–211.

Petropoulos, G. P., Ireland, G., Cass, A., Srivastava, P. K., 2015. Performance assessment of the SEVIRI evapotranspiration operational product: results over diverse mediterranean ecosystems. *IEEE Sensors Journal*, 15(6), 3412–3423.

Qi, J., Chehbouni, A., Huete, A. R., Kerr, Y. H., Sorooshian, S., 1994. A modified soil adjusted vegetation index. *Remote sensing of environment*, 48(2), 119–126.

Sharma, J., Prasad, R., Srivastava, P. K., Singh, S. K., Yadav, S. A., Pandey, D. K., 2025. Improved radar vegetation water content integration for SMAP soil moisture retrieval. *Remote Sensing Applications: Society and Environment*, 37, 101443.

Sharma, J., Prasad, R., Srivastava, P. K., Singh, S. K., Yadav, S. A., Yadav, V. P., 2021. Roughness characterization and disaggregation of coarse resolution SMAP soil moisture using single-channel algorithm. *Journal of Applied Remote Sensing*, 15(1), 014514–014514.

Srivastava, P. K., Han, D., Rico-Ramirez, M. A., O'Neill, P., Islam, T., Gupta, M., 2014. Assessment of SMOS soil moisture retrieval parameters using tau–omega algorithms for soil moisture deficit estimation. *Journal of Hydrology*, 519, 574–587.

Srivastava, P. K., Suman, S., Pandey, V., Gupta, M., Gupta, A., Gupta, D. K., Chaudhary, S. K., Singh, U., 2021. Concepts and methodologies for agricultural water management. *Agricultural water management*, Elsevier, 1–18.

Van de Griend, A. A., Wigneron, J.-P., 2004. The b-factor as a function of frequency and canopy type at H-polarization. *IEEE Transactions on Geoscience and Remote Sensing*, 42(4), 786–794.

Wang, L., Qu, J. J., 2009. Satellite remote sensing applications for surface soil moisture monitoring: A review. *Frontiers of Earth Science in China*, 3(2), 237–247.

West, R., 2014. Soil moisture active and passive mission (SMAP) L1B S0, L1C S0. *NASA, Washington, DC, USA*.

Zhao, W., Li, A., 2015. A comparison study on empirical microwave soil moisture downscaling methods based on the integration of microwave-optical/IR data on the Tibetan Plateau. *International Journal of Remote Sensing*, 36(19-20), 4986–5002.